Comparison of the efficiency of carbon dioxide capture by sorption-enhanced water–gas shift and palladium-based membranes for power and hydrogen production

J. Boon **(ECN)**
V. Spallina **(TU/e)**
Y.C. van Delft **(ECN)**
M. van Sint Annaland **(TU/e)**

May 2016
ECN-W--16-001

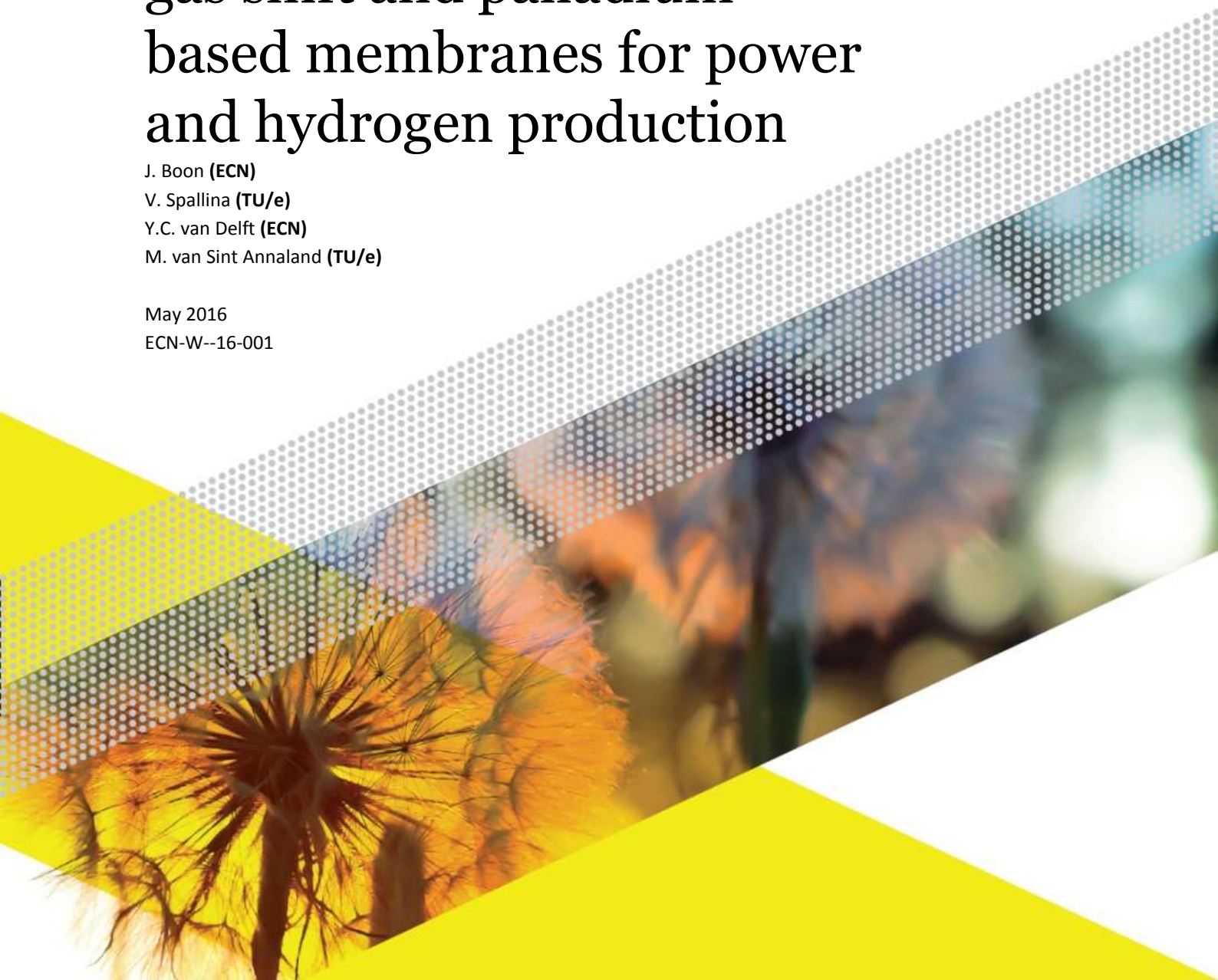

International Journal of Greenhouse Gas Control 50 (2016) 121–134

Contents lists available at ScienceDirect

International Journal of Greenhouse Gas Control

journal homepage: www.elsevier.com/locate/ijggc

Comparison of the efficiency of carbon dioxide capture by sorption-enhanced water–gas shift and palladium-based membranes for power and hydrogen production

Jurriaan Boon [a,b,*], Vincenzo Spallina [b], Yvonne van Delft [a], Martin van Sint Annaland [b]

[a] Sustainable Process Technology, ECN, P.O. Box 1, 1755ZG Petten, The Netherlands
[b] Chemical Process Intensification, TU/e, P.O. Box 513, 5600MB Eindhoven, The Netherlands

ARTICLE INFO

Article history:
Received 1 March 2016
Received in revised form 26 April 2016
Accepted 30 April 2016

Keywords:
High-temperature gas separation
Sorption-enhanced water–gas shift
Palladium-based membranes
Pre-combustion carbon dioxide capture
Thermodynamics
Exergy analysis

ABSTRACT

Pre-combustion capture of carbon dioxide requires the industrial separation of carbon dioxide from hydrogen-rich streams. The present study analyses the thermodynamic efficiency penalty of this separation step and the achievable carbon capture ratio, with particular focus on high-temperature separation technologies: sorption-enhanced water–gas shift (SEWGS) and palladium membranes. Twelve different cases have been simulated, starting from coal-derived syngas or from natural gas derived reformate, using carbon dioxide capture by conventional absorption, SEWGS, and palladium membranes, and producing hydrogen-rich fuel for power production or pure hydrogen. For the production of decarbonised fuel from coal syngas, SEWGS always yields the lowest efficiency penalty per unit of carbon dioxide captured. For the production of pure hydrogen from coal syngas, SEWGS has a significantly higher carbon capture ratio than the alternatives while palladium membranes yield the lowest efficiency penalty per unit of carbon dioxide captured. For the production of decarbonised fuel from natural gas reformate, SEWGS is the most efficient technology in terms of efficiency penalty. For the production of pure hydrogen from natural gas syngas, palladium membranes yield the lowest efficiency penalty.

1. Introduction

Pre-combustion capture of carbon dioxide comprises conversion of fuel into syngas, a mixture of predominantly carbon monoxide and hydrogen, and then reaction of the carbon monoxide with steam to carbon dioxide and more hydrogen via the water–gas shift reaction,

$$CO + H_2O \rightleftharpoons CO_2 + H_2 \quad \Delta H^{\circ}_{298\,K} = -41\,kJ\,mol^{-1} \tag{1}$$

After separation of the carbon dioxide, the hydrogen can be used without ensuing carbon dioxide emissions. The processes for the production of hydrogen and separation of carbon dioxide are by no means new. In fact, large quantities of hydrogen are presently produced industrially through these processes, mainly for various uses in chemical industry (Holladay et al., 2009; Häussinger et al., 2012, 2012). These conventional process schemes involve near ambient separation of carbon dioxide and hydrogen, e.g. by liquid scrubbing or pressure-swing adsorption, while the hydrogen is initially produced at high temperatures and frequently used at high temperatures, i.e. above 200 °C. In contrast, separation of carbon dioxide and hydrogen at high temperatures is possible with high-temperature sorbents or palladium-based membranes. These have consequently attracted a sustained academic interest over the last years, particularly in the framework of pre-combustion carbon dioxide capture (Yong et al., 2002; Dijkstra et al., 2011; Boon et al., 2012; Gallucci et al., 2013; Gazzani et al., 2013a,b, 2015; van Berkel et al., 2013; Wang et al., 2014; Atsonios et al., 2015; Jansen et al., 2015), aiming at the development of high-temperature technologies for the separation of carbon dioxide and hydrogen in general, and specifically for pre-combustion capture of carbon dioxide. Since the publication of the comparative results of the European FP6 Cachet project (Beavis, 2011), both sorption-enhanced water–gas shift (SEWGS) and palladium-based membranes have made considerable progress. A more detailed comparison on process efficiencies of pre-combustion carbon dioxide capture by SEWGS and palladium membranes is important to direct future research efforts in this field. The aim of the current work is to develop a theoretical framework for the efficiency-based comparison of pre-combustion carbon dioxide capture technologies.

* Corresponding author at: Sustainable Process Technology, ECN, P.O. Box 1, 1755ZG Petten, the Netherlands.
E-mail address: boon@ecn.nl (J. Boon).

http://dx.doi.org/10.1016/j.ijggc.2016.04.033
1750-5836/

Nomenclature

CCR	molar carbon capture ratio (–)
CO_xCR	molar carbon oxides capture ratio (–)
CP	carbon molar purity (–)
EBTF	European Benchmarking Task Force
F_m	mass flow rate ($kg\,s^{-1}$)
F_{mol}	molar flow rate ($kg\,s^{-1}$)
HP	hydrogen molar purity (–)
HRF	hydrogen recovery factor (–)
HTS	high-temperature water–gas shift
IGCC	integrated gasification combined cycle for coal
LHV	lower heating value ($MJ\,kg^{-1}$)
LTS	low-temperature water–gas shift
MDEA	*N*-methyl-diethanolamine $CH_3N(C_2H_4OH)_2$ for chemical absorption
p	pressure (Pa)
PEQ	pressure equalisation (in SEWGS)
PSA	pressure swing adsorption
Q	duty (MW)
Rep	repressurisation (in SEWGS)
S/C_{purge}	molar ratio of purge steam to carbon (as CO and CO_2) in the feed
S/C_{rinse}	molar ratio of rinse steam to carbon (as CO and CO_2) in the feed
SEWGS	sorption-enhanced water–gas shift
T	temperature (K)
W	work (MW)
WGS	water–gas shift
y	mole fraction (–)
η	efficiency (–)

Starting with syngas from either coal gasification or natural gas reforming, the present study quantifies the work of the separation of carbon dioxide for conventional low temperature technology (Selexol, MDEA) on the one hand and for sorption-enhanced water–gas shift (SEWGS) and palladium-based membranes on the other. (The membranes are used in separator modules, membrane reactors are outside the scope of this work.) Initially, a total of twelve different process schemes are discussed to produce various qualities of hydrogen while capturing carbon dioxide, including schemes with conventional low-temperature separations as well as schemes with high-temperature separation. Then, this paper discusses the thermodynamic framework for assessment of the work required for the separation of carbon dioxide and hydrogen. The advantage of high-temperature separations will be assessed in terms of the efficiencies according to the first and second law of thermodynamics.

2. Methods

2.1. Description of the plants

Four basic process options are considered in this work,

- low-temperature separation by Selexol,
- low-temperature separation by methyl diethanolamine solution (MDEA),
- high-temperature separation by sorption-enhanced water–gas shift (SEWGS), and
- high-temperature separation by palladium-based membranes.

The three process schemes are used with syngas either from coal gasification or natural gas reforming. With respect to the feeds streams, shown in Table 1, the main difference is in the carbon oxides content. Coal syngas has a high carbon content (> 20 mol% CO + CO_2, note that the syngas from a Shell gasifier has already undergone a first stage of high-temperature water–gas shift reaction) while natural gas derived syngas has a lower carbon oxides content (< 15 mol% CO + CO_2). This is a principal difference, because the partial pressure of carbon dioxide in the feed determines the driving force for capture in Selexol, MDEA, and SEWGS, and thereby to a large extent the performance of the capture processes. Therefore, the obtained results for coal syngas also represent the potential to separate carbon dioxide from industrial gases with high carbon oxides content, such as blast furnace gas in steelworks and producer gas from biomass gasification, possibly after compression (Gielen, 2003; Carbo et al., 2011; Gazzani et al., 2015). Similarly, the results for natural gas derived syngas indicate the potential to separate carbon dioxide from industrial gases with low carbon oxides content, such as coke oven gas in steelworks (Gazzani et al., 2015).

Table 1
Syngas feed compositions considered in this work.

		Coal gasification	Natural gas reforming
Pressure	bar	40	29
Temperature	°C	400	400
Composition	mole fraction		
H_2		0.36	0.49
CO_2		0.24	0.084
H_2O		0.30	0.34
CO		0.050	0.056
CH_4			0.033
N_2		0.044	0.002
Ar		0.004	
H_2S		0.001	

Note that sulphur, specifically hydrogen sulphide, is not accounted for quantitatively, except for the Rectisol process. For SEWGS, hydrogen sulphide will be co-captured with carbon dioxide and leave the column with the carbon dioxide product in the purge step (van Dijk et al., 2011; Boon et al., 2015a).

Table 2 shows the considered process routes. The schemes have been designed to produce two different qualities of hydrogen, and a carbon dioxide stream of sufficient purity for sequestration (Table 3). Pure hydrogen product (>99.9 vol.%) has strict purity constraints and can be produced by either a conventional pressure swing adsorption system (Kohl and Nielsen, 1997), or with palladium membranes by using steam sweep that can be readily condensed. In contrast, there is no strict purity constraint for the hydrogen product in case it is used as fuel, e.g. in a pre-combustion carbon dioxide capture scheme. In fact, the hydrogen product requires dilution with inert (nitrogen when available, in case of coal syngas, or steam) before its use as fuel in a hydrogen-rich fuelled gas turbine for power production (Gazzani et al., 2013a,b). Gazzani et al. (2014a) have well addressed and discussed the fuel specifications for the use of hydrogen as gas turbine fuel in pre-combustion carbon dioxide capture schemes. The carbon dioxide purity constraint for compression and sequestration is taken from the European Benchmarking Task Force to be 90 vol.%, yet with more stringent purity constraints for many relevant impurities (Franco et al., 2009). The pressure for sequestration is assumed to be 110 bar(a).

2.1.1. Water–gas shift

The water–gas shift reaction (1) is used to convert carbon monoxide with steam into additional hydrogen product. Three types of industrially mature water–gas shift processes are employed in the schemes above: sour WGS, high-temperature WGS (HTS), and low-temperature WGS (LTS) (Newsome, 1980; Carbo et al., 2009). First important distinction between the processes is in terms of the sulphur content and the corresponding

Table 2
Process routes considered.

Case	Syngas	Technology	Product	Byproduct
I	Coal	Sour WGS, Selexol	H_2 fuel	CO_2
II	Coal	Sour WGS, Selexol, PSA	H_2	CO_2
III	Coal	Sour WGS, SEWGS	H_2 fuel	CO_2
IV	Coal	Sour WGS, SEWGS, PSA	H_2	CO_2
V	Coal	Rectisol, HTS and membrane (sequentially in 3 stages, N_2 sweep), cryogenic	H_2—N_2	CO_2
VI	Coal	Rectisol, HTS and membrane (sequentially in 3 stages, H_2O sweep), cryogenic	H_2	CO_2
VII	NG	HTS, LTS, MDEA	H_2 fuel	CO_2
VIII	NG	HTS, LTS, MDEA, PSA	H_2	CO_2
IX	NG	SEWGS	H_2 fuel	CO_2
X	NG	SEWGS, PSA	H_2	CO_2
XI	NG	HTS and membrane (sequentially in 3 stages, H_2O sweep), cryogenic	H_2—H_2O	CO_2
XII	NG	HTS and membrane (sequentially in 3 stages, H_2O sweep), cryogenic	H_2	CO_2

catalyst stability, the second distinction is in the operating temperature regime. In sour water–gas shift, high-sulphur syngas is converted using sulphided catalysts (typically cobalt molybdenum sulphide). A fairly high level of sulphur is required in the syngas in order for the catalyst to remain in the sulphided state and the reactor operates in the range of 244–250 °C inlet and up to 480 °C outlet temperature. The HTS process at 350 °C inlet and up to 395 °C outlet temperature uses iron oxide based catalysts and can tolerate a fair amount of sulphur with only a mild reduction in activity (Boon et al., 2009; van Dijk et al., 2014). The LTS process requires sulphur-free syngas (<0.1 ppmv) and operates from 200 °C inlet to 217 °C outlet temperature.

The low-temperature carbon dioxide capture cases (I, II, VII, and VIII) use conventional technology (Selexol, MDEA) and represent state of the art. Advanced split flow configuration of the water–gas shift section could significantly lower the steam demand, albeit at the cost of an increased number of reactors and total catalyst volume (Carbo et al., 2009), which is not considered here.

2.1.2. Selexol, MDEA

Absorption is widely used industrially for the separation of acid species (such as carbon dioxide and hydrogen sulphide) from gas streams (Kohl and Nielsen, 1997; Boll et al., 2000; Jansen et al., 2015). The gas phase is contacted with a liquid which either dissolves (physical absorption) or chemically binds (chemical absorption) the acid gases. Regeneration is done by pressure swing or temperature swing (reboiling). At high partial pressures, physical solvents outperform chemical solvents, while the reverse is true for low partial pressures (Boll et al., 2000). As state of the art, physical absorption by Selexol is selected for the capture of carbon dioxide and hydrogen sulphide from coal syngas (case I and II) and chemical absorption by MDEA is selected for the capture of carbon dioxide from natural gas reformate (case VII and VIII).

The Selexol section for separation of carbon dioxide and hydrogen sulphide is modelled after Spallina et al. (2014). The energy consumption is 189 kJ $kg^{-1}_{CO_2\text{-rich}}$ for pumping and 303 kJ $kg^{-1}_{CO_2\text{-rich}}$ at 200 °C for the reboiler. Compression of the carbon dioxide product consumes 252 kJ $kg^{-1}_{CO_2\text{-rich}}$ of electricity. The MDEA section for separation of carbon dioxide is modelled after Chiesa et al. (2013). The energy consumption is 84 kJ $kg^{-1}_{CO_2\text{-rich}}$ of electricity for pumping and 887 kJ $kg^{-1}_{CO_2\text{-rich}}$ at 200 °C for the reboiler. Compression of the carbon dioxide product is modelled according to the EBTF (Section 2.1.8).

Table 3
Product stream specifications (Franco et al., 2009; Gazzani et al., 2013a,b).

Species		Hydrogen	Hydrogen-rich fuel	Carbon dioxide for sequestration
H_2	mol%	99.9	<60	<4
CO	mol%			<0.2
CO_2	mol%			>90
H_2O	mol%			
N_2	mol%			<4
CH_4	mol%			<2
H_2S	ppmv		<20	<200
Temperature	°C		200–350	25

2.1.3. Sorption-enhanced water–gas shift

Sorption-enhanced water–gas shift (SEWGS) combines the water–gas shift reaction with in situ adsorption of carbon dioxide on potassium-promoted hydrotalcite and thereby allows production of hot, high pressure hydrogen from syngas in a single unit operation (Hufton et al., 1999; Cobden et al., 2007; van Selow et al., 2009). SEWGS is a cyclic process, that comprises high pressure adsorption and rinse, pressure equalisation, and low pressure purge. The cyclic stability of the SEWGS process for 2000 cycles has been demonstrated (van Selow et al., 2013; Jansen et al., 2013). Currently, a SEWGS pilot installation for the capture of 14 t d^{-1} of carbon dioxide is being constructed as part of the Stepwise project in Luleå, Sweden, in the European H2020 LCE programme (Stepwise, 2016).

In SEWGS, steam is added in the rinse (high-pressure rinse steam, expressed on a molar basis as S/C_{rinse}) and in the purge (low-pressure purge steam, expressed on a molar basis as S/C_{purge}). In an earlier work (Boon et al., 2015a), extensive results have been presented of a SEWGS cycle design study, based on recently developed expressions for the interaction of carbon dioxide and steam with potassium-promoted hydrotalcite at high pressure (Boon et al., 2014), yielding a SEWGS cycle that consumes significantly less steam than cycle designs previously reported in literature. For IGCC syngas, a SEWGS system of 9 columns was presented which could reach a carbon capture ratio and carbon dioxide purity of 95% and 99%, respectively, with S/C_{rinse} of 0.03 and S/C_{purge} of 0.08. For the performance in a carbon dioxide capture process, it is important to stress that the sorbent itself can perform substantial water–gas shift conversions (it requires no additional catalyst), and that it is able to capture hydrogen sulphide together with carbon dioxide (van Dijk et al., 2011; Gazzani et al., 2013a). Also, SEWGS easily achieves very high capture ratios.

Based on these results, new SEWGS cycle designs have been studied in the present work using the previously presented sorption-enhanced reactor model (Reijers et al., 2009; Boon et al., 2014). The S/C_{purge} has been fixed at 0.1 in order to achieve a carbon dioxide capture ratio of around 98%. The main parameter variations in the current study are S/C_{rinse} and the number of pressure equalisations. The former mainly affects the carbon dioxide purity while it represents the largest work lost. The latter also strongly affects the carbon dioxide purity, while it implies a number of columns and consequently strongly determines the required capital expenditure. The reduction in pressure equalisations from 3 to 2 and 1 reduces the number of SEWGS columns from 9 to 8 and 7,

respectively. Thus, the steam consumption and number of pressure equalisations can be varied in order to achieve the desired carbon dioxide purity. Simulations for coal syngas have been extended from the previous study (Boon et al., 2015a), while new simulations have been performed for natural gas reformate.

2.1.4. Palladium-based membranes

Hydrogen is soluble in palladium metal and dense palladium membranes can have an extremely high permselectivity for hydrogen (only related to defects and capping). Therefore, metallic palladium and palladium alloy membranes have received a great deal of interest from researchers worldwide (Paglieri and Way, 2002; Basile et al., 2008; Yun and Oyama, 2011; Gallucci et al., 2013). Palladium based membranes are currently in use for the production of hydrogen in niche markets and their economic potential extends to chemical industry, pre-combustion carbon dioxide capture, and the production of ultrapure hydrogen (Paglieri and Way, 2002; Ockwig and Nenoff, 2007; Gazzani et al., 2014b; Atsonios et al., 2015; Gazzani and Manzolini, 2015). The stability of palladium membranes in experiments of up to a year is discussed by Gallucci et al. (2013). In previous studies under the Dutch CATO-2 programme, commercially available palladium membranes have been benchmarked (Boon et al., 2013), the mass transfer resistance in the membrane support because of the use of sweep gas (Boon et al., 2012), and the impact of inhibition by syngas species was quantified under relevant, high pressure, conditions (Li et al., 2010; Boon et al., 2015b). Although palladium-based membranes can be integrated in water–gas shift reactors (Bracht et al., 1997; Li et al., 2012) or even in reformers (Tiemersma et al., 2006; Patil et al., 2007; Li et al., 2011; van Berkel et al., 2013), a staged approach is adopted mainly because of techno-economic reasons and operability issues (Gazzani and Manzolini, 2015; Hudiono et al., 2015): three consecutive HTS reactors are each followed by membrane modules for the recovery of hydrogen.

In the current study, pure palladium membranes are used at 350 °C, which require sub-ppm level hydrogen sulphide and consequently a Rectisol desulphurisation process is installed for coal syngas (Case V and VI) (Gazzani and Manzolini, 2015). The driving force for hydrogen permeation is related to the difference in hydrogen partial pressure over the membrane, and consequently the use of sweep gas improves the performance. In the current cases, a high-pressure counter-current sweep of nitrogen or steam is assumed, related to the final pressure at which the hydrogen needs to be produced. This is in line with a recent study by Atsonios et al. (2015), who showed an increase in system efficiency with increasing sweep gas pressure, at the expense of a higher required membrane surface area. Sweep gas improves the driving force for permeation, but induces additional resistance to mass transfer, especially at higher pressures (Boon et al., 2012). The net effect of sweep on the transmembrane flux remains strongly positive and the use of sweep gas is to be preferred over hydrogen recompression.

For the membrane modules, the hydrogen recovery factor is a design variable. An increase in the hydrogen recovery factor entails an increase in the required membrane surface area as well as an increase in the amount of sweep gas. The former is outside the scope of the current study, whereas the latter is an important factor determining the efficiency. On the one hand a higher sweep flow rate improves the hydrogen recovery factor which leads to a higher cold gas efficiency, but on the other it requires either more steam to be raised or nitrogen to be compressed which lowers the overall efficiency. A sensitivity study was performed on the hydrogen recovery factor, varying the hydrogen recovery per module in the range of 70–95%. The overall hydrogen recovery factor thereby varied between 97% and 99.95%, which is always higher than conventional technologies and SEWGS achieve. The permeance for non-hydrogen species is assumed to be negligible – neglecting membrane defects or leaks via the membrane seals. The only impurity in the hydrogen product thus originates from the sweep gas used (which is steam in cases VI and XII, for pure hydrogen product). It is assumed that steam can be condensed and removed at 25 °C but if necessary cooled systems can achieve lower dew points at relatively little additional work. The sweep flow rate is adjusted such that the partial pressure difference over the membrane (at both the feed inlet side and the sweep inlet side) is at least 10% of the feed side partial pressure of hydrogen, in order to ensure a high driving force for permeation and a low required membrane surface area.

2.1.5. Pressure swing adsorption

State of the art technology for the production of pure hydrogen is pressure swing adsorption (PSA) (Kohl and Nielsen, 1997). It produces a high pressure stream of high purity hydrogen and a low pressure stream of tail gas. The tail gas is accounted for in terms of its lower heating value, see Section 2.3.2. The PSA system is modelled according to industrial practice using a hydrogen recovery of 76.2% and a hydrogen purity of 99.9996 mol% (Kohl and Nielsen, 1997).

2.1.6. Rectisol desulphurisation

As discussed, palladium membranes require desulphurisation upfront. Rectisol (cryogenic methanol physical absorption) is used (Kohl and Nielsen, 1997). As discussed by Gazzani and Manzolini (2015), the Rectisol process can be tailored for a high selectivity for hydrogen sulphide over carbon dioxide which is important in pre-combustion carbon dioxide capture schemes. A power consumption of 25 MJ $kg^{-1}_{H_2S}$ and reboiler duty of 63 MJ $kg^{-1}_{H_2S}$ (at 70 °C) are required (Gazzani and Manzolini, 2015).

2.1.7. Cryogenic purification of carbon dioxide

The retentate remaining after the last membrane separation stage, with a hydrogen recovery factor of 97–99.95% (Section 2.1.4), still contains a significant amount of hydrogen, but also carbon monoxide, and possibly methane. This represents a significant energy content but recovery is not feasible with membranes. Instead, cryogenic purification of carbon dioxide is used (Atsonios et al., 2013). This allows recovery of the energy content as well as achieving the specified carbon dioxide purity. The power consumption for cryogenic cooling is estimated at 5.4 kJ $kg^{-1}_{CO_2\text{-rich}}$ (Chiesa et al., 2011).

2.1.8. Compression and condensation

Depending on the separation technology of choice, the carbon dioxide product is delivered either at atmospheric pressure (MDEA, SEWGS) or at elevated pressure. The installation of any carbon dioxide capture technology presupposes a destination for the carbon dioxide, other than emission to the atmosphere. The carbon dioxide stream is therefore compressed to a pressure of 110 bar(a), creating a common basis for comparing the technologies. Compression stages and interstage cooling are modelled according to EBTF recommendations (Franco et al., 2009), except for Selexol where a literature value is used (Section 2.1.2).

2.2. Flowsheeting and equation of state

Flowsheets for the cases outlined above are briefly summarised in Fig. 1. The flowsheets are modelled in Aspen Plus V8.4, using the Peng–Robinson cubic equation of state, which is particularly suitable for light gases and at high temperature and pressure (Peng and Robinson, 1976).

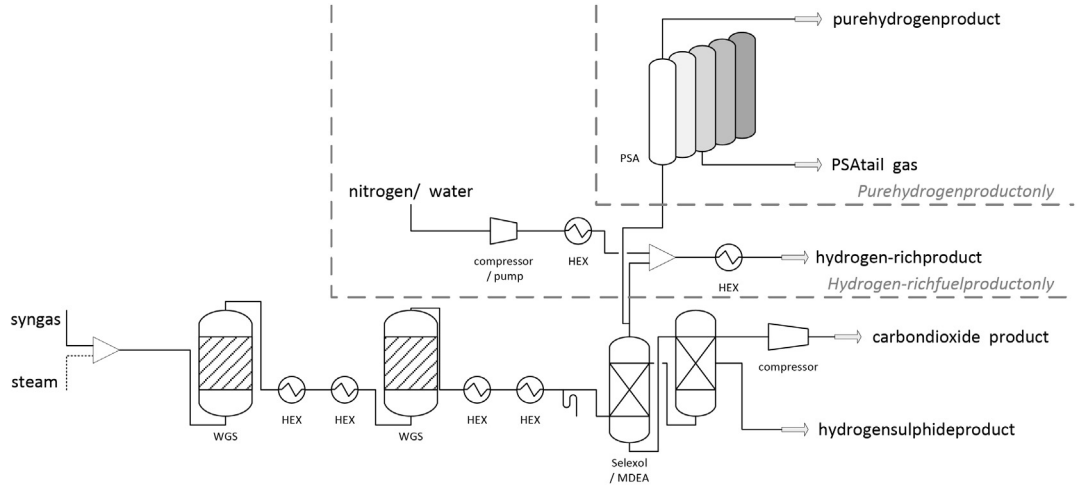

(a) Conventional separation processes Selexol and MDEA

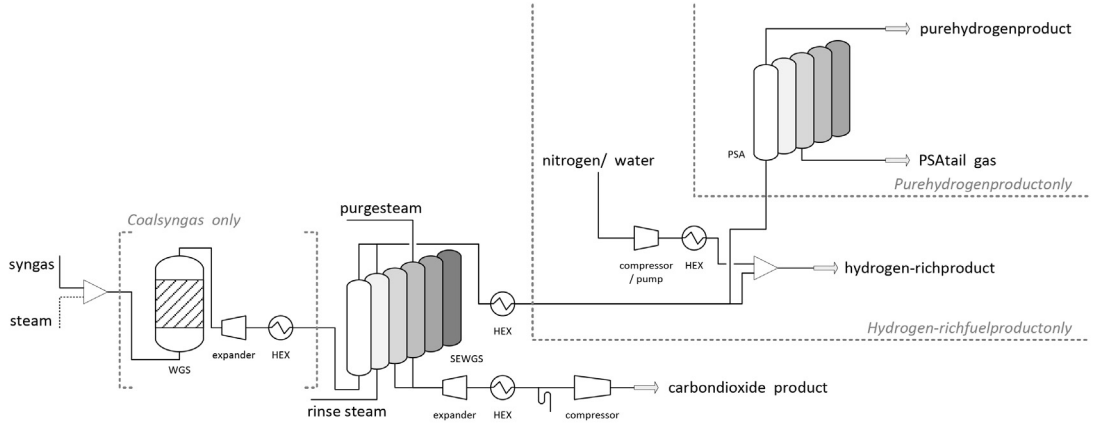

(b) SEWGS integrated water-gas shift and separation

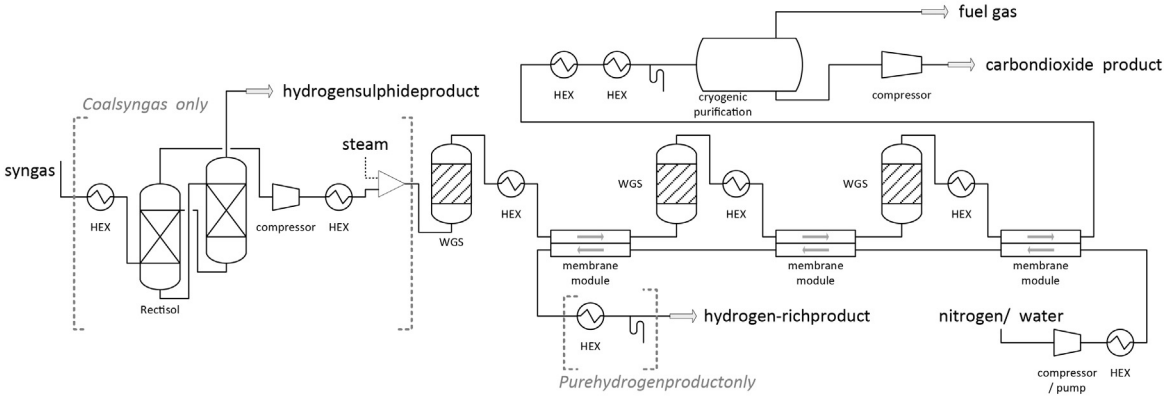

(c) Palladium-based membrane separation

Fig. 1. Process flow diagrams as discussed in Section 2.3, dotted lines indicate optional unit operations and process routes, depending on the case.

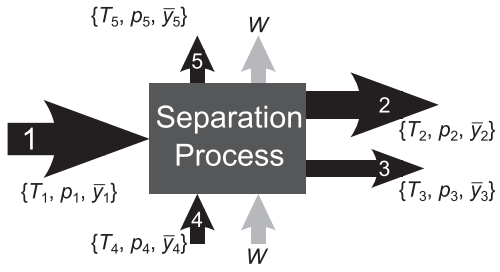

Fig. 2. Generic separation process, separating stream (1) into streams (2) and (3) by means of additional stream (4) and net work (ΔW), producing side product (5).

2.3. Process systems engineering

Fig. 2 shows a generic separation process. A single gas stream (1), of given temperature, pressure, and composition, is separated into two different gas streams: hydrogen rich (2), and carbon dioxide rich (3). The separation process requires and performs work (W), and, depending on the processes, additional process streams (4, e.g., steam, nitrogen). For several of the cases discussed below, a side product stream (5) of PSA tail gas is produced as well.

2.3.1. Process efficiency and steam consumption

The efficiency of the process is expressed in terms of the lower heating values (LHV) of the feed and product streams, i.e. cold gas efficiency. It is important to note that the cases for electricity production have also been modelled based on LHV efficiency for the conversion of fuel to power. Thus, specific modelling of a cooled gas turbine, which has been presented in literature (Chiesa and Macchi, 2004; Gazzani et al., 2014a) and is outside the scope of the current work, can be circumvented. Three efficiencies are defined accordingly:

$$\eta_0 = \frac{\mathrm{LHV}_{\mathrm{H_2\ \ product}} F_{\mathrm{m,H_2\ \ product}}}{\mathrm{LHV}_{\mathrm{feed}} F_{\mathrm{m,feed}}} \tag{2}$$

$$\eta_1 = \frac{\mathrm{LHV}_{\mathrm{H_2\ \ product}} F_{\mathrm{m,H_2\ \ product}} + \eta_{\mathrm{by\text{-}product}} \mathrm{LHV}_{\mathrm{by\text{-}product}} F_{\mathrm{m,by\text{-}product}}}{\mathrm{LHV}_{\mathrm{feed}} F_{\mathrm{m,feed}}} \tag{3}$$

$$\eta_2 = \frac{\mathrm{LHV}_{\mathrm{H_2\ \ product}} F_{\mathrm{m,H_2\ \ product}} + \eta_{\mathrm{by\text{-}product}} \mathrm{LHV}_{\mathrm{by\text{-}product}} F_{\mathrm{m,by\text{-}product}} - \Delta W}{\mathrm{LHV}_{\mathrm{feed}} F_{\mathrm{m,feed}}} \tag{4}$$

Thus, η_0 is defined as the cold gas efficiency, based on lower heating value of the hydrogen-rich product stream divided by the lower heating value of the syngas input. It is a measure to what extent the energy content in the syngas is preserved in the hydrogen-rich product. Similarly, η_1 represents the cold gas efficiency while taking into account the energy content of the by-product that is produced, which can be utilised as fuel (Section 2.3.3). Finally, η_2 is the theoretical net efficiency, accounting for the net work performed by the system in the process (Fig. 2), e.g. the consumption or production of steam and electricity. (Note that the theoretical net efficiency does not represent the efficiency according to the second law of thermodynamics.) The net efficiency thereby provides a measure of the required work for the conversion of carbon monoxide and the separation of carbon dioxide from the syngas.

Apart from the efficiencies, the performance of the processes is quantified through a number of key metrics: the hydrogen recovery factor (HRF), hydrogen purity (HP), carbon capture ratio (CCR), and carbon purity (CP),

$$\mathrm{HRF} = \frac{y_{\mathrm{H_2,H_2\ \ product}} F_{\mathrm{mol,H_2\ \ product}}}{\left(y_{\mathrm{H_2}} + y_{\mathrm{CO}}\right)_{\mathrm{feed}} F_{\mathrm{mol,feed}}} \tag{5}$$

$$\mathrm{HP} = y_{\mathrm{H_2,H_2\ \ product}} \tag{6}$$

$$\mathrm{CCR} = \frac{\left(y_{\mathrm{CO_2}} + y_{\mathrm{CO}} + y_{\mathrm{CH_4}}\right)_{\mathrm{feed}} F_{\mathrm{mol,CO_2\ \ product}}}{\left(y_{\mathrm{CO_2}} + y_{\mathrm{CO}} + y_{\mathrm{CH_4}}\right)_{\mathrm{feed}} F_{\mathrm{mol,feed}}} \tag{7}$$

$$\mathrm{CO_x CR} = \frac{\left(y_{\mathrm{CO_2}} + y_{\mathrm{CO}}\right)_{\mathrm{feed}} F_{\mathrm{mol,CO_2\ \ product}}}{\left(y_{\mathrm{CO_2}} + y_{\mathrm{CO}}\right)_{\mathrm{feed}} F_{\mathrm{mol,feed}}} \tag{8}$$

$$\mathrm{CP} = y_{\mathrm{CO_2,CO_2\ \ product}} \tag{9}$$

Since all remaining carbon monoxide and methane will be oxidised to carbon dioxide in downstream processes, they are accounted for in the carbon capture rate (Eq. (7)). The capture ratio of carbon oxides ($\mathrm{CO_x CR}$, Eq. (8)) serves to assess the capture of carbon dioxide and carbon monoxide, without accounting for the unconverted methane in the natural gas cases.

2.3.2. Work of separation

The work of separation is performed by equipment (electricity) and streams (steam) in the process. The work is done by the pressure of the feed, by the compression, and by the additional process streams involved. With Selexol, MDEA, and SEWGS, pressure swing is used to capture and release the carbon dioxide from the process stream, which means that the carbon dioxide is produced at low pressure. With palladium membranes, in contrast, the feed partial pressure produces the driving force for permeation of the hydrogen across the membrane and it is the hydrogen which is produced at lower pressure. The additional stream (4) in Fig. 2 can be steam (SEWGS rinse gas, SEWGS purge gas, membrane sweep gas) or nitrogen (membrane sweep gas). Side product (5) can be PSA tail gas or the side product obtained in cryogenic purification of carbon dioxide, both of which have significant calorific value.

Heat to work efficiencies are calculated according to basic Carnot and Lorentz cycles for heat engines, as shown in Fig. 3. The Carnot cycle operates between a *fixed* high temperature stream and a fixed low temperature sink, and its efficiency represents the maximum efficiency for converting heat into power. The Lorentz cycle operates between a *cooled* high temperature stream and a constant low temperature sink. Their respective maximum efficiencies are (Lee and Kim, 1992),

$$\eta_C = 1 - \frac{T_{\mathrm{L}}}{T_{\mathrm{H}}} \quad \text{Carnot cycle} \tag{10}$$

$$\eta_L = 1 - \frac{T_{\mathrm{L}}}{\sqrt{T_{\mathrm{H}} T_{\mathrm{L}}}} \quad \text{Lorentz cycle} \tag{11}$$

With the basic thermodynamic cycles, the efficiencies for converting heat into work are calculated for high temperature (>350 °C, Figs. 4 and 5) and similarly for medium temperature heat exchangers (150–350 °C) in the process. For all cases, the stream with the highest temperature is cooled and consequently the resulting heat engine corresponds to the Lorentz cycle. The lower temperature stages typically have an efficiency in between the maximum Carnot efficiency and the Lorentz efficiency. The efficiency for converting heat duty to work is therefore calculated by taking the arithmetic mean between Lorentz–Carnot and Lorentz–Lorentz cycles efficiencies. This way, the detailed simulation of the entire plant (including concomitant choices and assumptions) is avoided while a realistic performance of a derived steam cycle operated with the heat sources of the plant is taken into account: (i) different

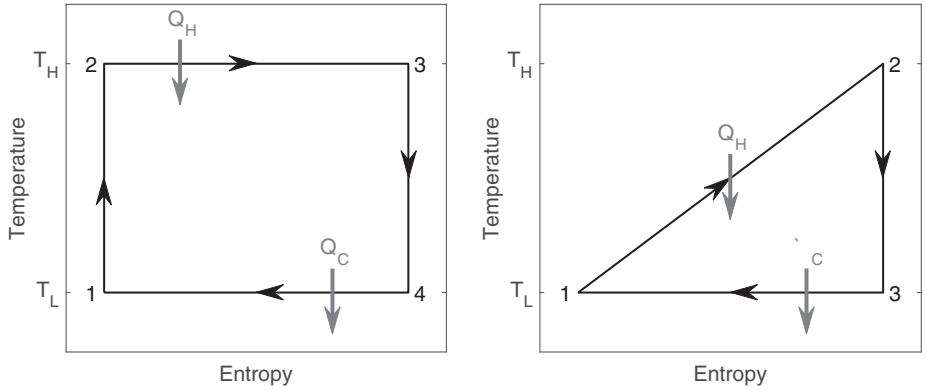

Fig. 3. Temperature–entropy diagram for a Carnot cycle (1-2-3-4) heat engine (left) and a Lorentz cycle (1-2-3) heat engine (right).

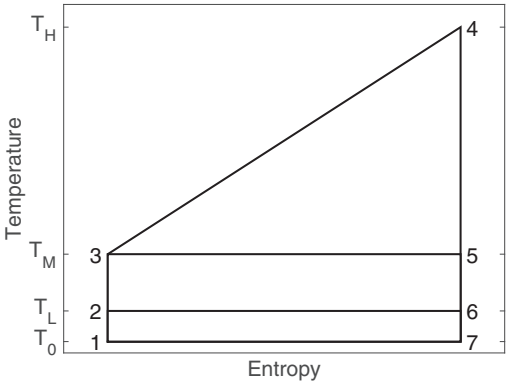

Fig. 4. Temperature–entropy diagram for heat recovery by high-temperature heat exchanger: Lorentz cycle (3-4-5) and two Carnot cycles (2-3-5-6, 1-2-6-7).

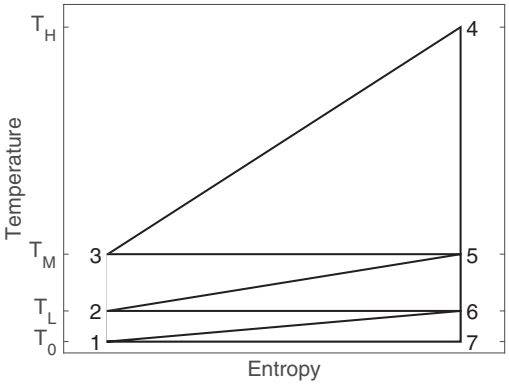

Fig. 5. Temperature–entropy diagram for heat recovery by high-temperature heat exchanger: three Lorentz cycles (3-4-5, 2-5-6, 1-6-7).

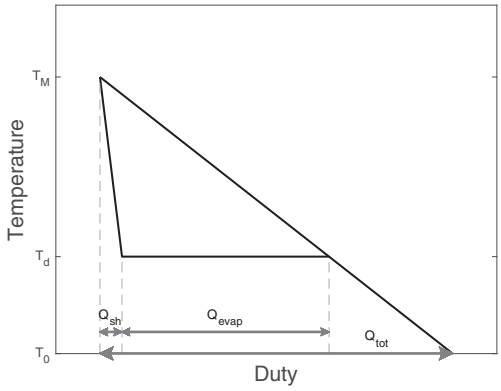

Fig. 6. Temperature–duty diagram for the work corresponding to steam added to the process.

steam streams at high, intermediate, and low pressure are generated during heat recovery; (ii) the Lorentz cycle does not take into account that steam production occurs through evaporation and super-heating; and (iii) for example a stream at 650 °C which is cooled down to ambient temperature would achieve a Carnot efficiency of 69%, a Lorentz efficiency of 44% and based on our methodology will achieve an overall efficiency of 56% which is in line with state of the art steam cycle performance (Franco and Russo, 2002). The cases and typical efficiencies are summarised in Table 4.

Added steam, as opposed to steam used for heating, is accounted for in terms of lost work (which could otherwise have been performed by the steam in a steam turbine). The amount of work that steam of T_M can perform depends on its temperature and pressure (through the dew point T_d). As shown in Fig. 6, the lost work by steam addition is quantified from the heat duty to raise the steam (Q_s) through Lorentz cycle efficiency,

$$\eta_s = \frac{(T_s - T_0)(1 - (T_0/\sqrt{T_s T_0})) - (T_d - T_0)\left(1 - (T_0/\sqrt{T_d T_0})\right)}{T_s - T_d} \quad (12)$$

The remaining work is electric. The used compressors and expanders, including refrigeration, were discussed in Section 2.1.8.

2.3.3. Utilisation of by-product

In several of the cases, a by-product stream of significant calorific value is produced. It is assumed that such a stream can

Table 4
Typical efficiency calculations for high-temperature heat exchangers (HTHEX), and medium-temperature heat exchangers (MTHEX) using Eqs. (10) and (11).

Cases		T_H (°C)	T_M (°C)	T_L (°C)	T_0 (°C)	η_{L1}	η_{L2}	η_{L3}	η_{C2}	η_{C3}	η	Formulae
HTHEX	max	480	350	150	15	0.090	0.176	0.175	0.321	0.319	0.579	$\eta = \eta_{L1} + \eta_{C2} + \eta_{C3} - \eta_{L1}\eta_{C2} - \eta_{L1}\eta_{C3} - \eta_{C2}\eta_{C3} + \eta_{L1}\eta_{C2}\eta_{C3}$
	min										0.381	$\eta = \eta_{L1} + \eta_{L2} + \eta_{L3} - \eta_{L1}\eta_{L2} - \eta_{L1}\eta_{L3} - \eta_{L2}\eta_{L3} + \eta_{L1}\eta_{L2}\eta_{L3}$
MTHEX	max		350	150	15		0.176	0.175	0.321	0.319	0.439	$\eta = \eta_{L2} + \eta_{C3} - \eta_{L2}\eta_{C3}$
	min										0.320	$\eta = \eta_{L2} + \eta_{L3} - \eta_{L2}\eta_{L3}$

Table 5
Major results summarised for the selected cases, metrics defined in Section 2.3.1.

Case	Feed	Technology	Product	η_0	η_1	η_2	HRF	HP	CCR	CO_xCR	CP
I	Coal	Selexol	Fuel	0.89	0.89	0.76	0.966	0.600	0.918	0.918	0.985
II			H_2	0.66	0.76	0.67	0.736	1.000	0.918	0.918	0.985
III		SEWGS	Fuel	0.87	0.87	0.75	0.964	0.600	0.978	0.978	0.961
IV			H_2	0.65	0.75	0.65	0.735	1.000	0.978	0.978	0.961
V		Membranes	Fuel	0.86	0.86	0.73	0.985	0.380	0.902	0.902	0.964
VI			H_2	0.86	0.88	0.76	0.968	0.999	0.902	0.902	0.964
VII	Natural gas	MDEA	Fuel	0.98	0.98	0.94	0.989	0.600	0.759	0.939	0.969
VIII			H_2	0.62	0.78	0.78	0.754	1.000	0.759	0.939	0.969
IX		SEWGS	Fuel	0.98	0.98	0.95	0.987	0.600	0.765	0.946	0.963
X			H_2	0.62	0.78	0.79	0.752	1.000	0.765	0.946	0.963
XI		Membranes	Fuel	0.98	0.98	0.88	0.998	0.388	0.760	0.940	0.990
XII			H_2	0.81	0.89	0.88	0.989	0.999	0.760	0.940	0.990

be converted into work via a steam boiler, using a state of the art efficiency of 45% LHV (Cau et al., 2014).

2.3.4. Work of separation

As stated in the introduction, this study aims to develop a framework for the evaluation of different technologies for pre-combustion carbon dioxide capture. The common denominator in the evaluation is the work of separation. Using the efficiencies derived above in the flowsheeting work, the heat demand or production of unit operations (Q), the steam added to the process (Q_s), and the utilisation of by-products (LHV) can all be converted to work:

$$W = \eta Q \tag{13}$$

$$W_s = \eta_s Q_s \tag{14}$$

$$W = \eta_{\text{by-product}} \text{LHV}_{\text{by-product}} F_{\text{m,by-product}} \tag{15}$$

3. Results

Flowsheets for the twelve cases have been modelled, all resulting in meeting the product specifications of hydrogen product and carbon dioxide product (Table 3). The major results are summarised in Table 5. First, the results for the different cases are discussed.

3.1. Conventional absorption technology

In case I and II, the Selexol process achieves a CCR of 92%. In case VII and VIII, at lower carbon dioxide partial pressure, and with a relatively high methane content, a CCR of 76% is reached with MDEA (see discussion below).

3.2. Sorption-enhanced water–gas shift

The sorption-enhanced water–gas shift (SEWGS) process in this study has been designed for a specified carbon dioxide purity. It has been shown that SEWGS can readily achieve very high carbon capture ratios (Boon et al., 2015a; Walspurger et al., 2015). The present work is based on the performance of the Alkasorb sorbent as developed by ECN; adopting the novel Alkasorb+ would further improve the SEWGS performance (Jansen et al., 2013).

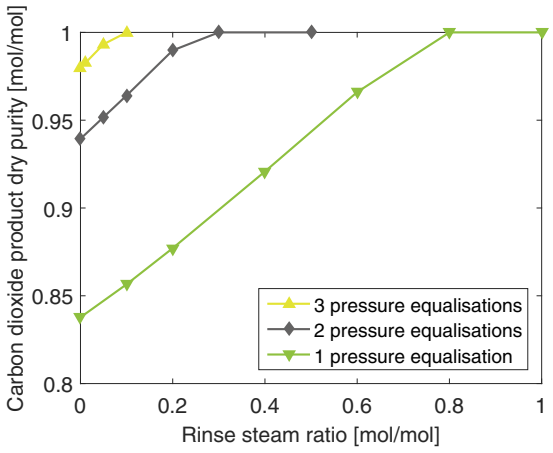

Fig. 7. SEWGS performance, carbon dioxide product dry purity versus rinse steam consumption for 3, 2, and 1 pressure equalisation with coal syngas after pre-shift and $S/C_{purge} = 0.1$.

Results of the carbon dioxide purity from SEWGS cycle simulations are shown in Fig. 7. Clearly, both the rinse steam amount and the number of pressure equalisations strongly affect the carbon dioxide purity. The target purity of 96 mol% can be achieved with 8 columns using $S/C_{rinse} = 0.1$ and $S/C_{purge} = 0.1$. The corresponding schedule is shown in Fig. 8. An interesting alternative would be to use a 9 column configuration, and no or negligible rinse (Fig. 7). Clearly this would significantly improve the work of carbon dioxide separation, at the expense however of an increased cost of equipment. Since the SEWGS process without rinse has not yet been experimentally demonstrated, it is not used in the system evaluation but considered as a promising future development.

SEWGS simulations for the natural gas reformate have recently been presented by Walspurger et al. (2015) and are briefly summarised in Fig. 9. The lower partial pressure of carbon oxides in the natural gas reformate translates into a higher steam consumption. The required carbon dioxide purity is reached at $S/C_{rinse} = 0.5$ and

Column	1/4			1/8		1/16	1/16	1/16	1/4				1/16	1/16	1/16
1	Adsorption			Rinse		PEQ1 ↓	PEQ2 ↓	Blowdn	Purge				PEQ2 ↑	PEQ1 ↑	Rep
2	PEQ1 ↑	Rep	Adsorption			Rinse		PEQ1 ↓	PEQ2 ↓	Blowdn	Purge				PEQ2 ↑
3	Blowdn	Purge		Adsorption				Rinse		PEQ1 ↓	PEQ2 ↓	Blowdn	Purge		
4	Rinse		PEQ1 ↓	PEQ2 ↓	Blowdn	Purge	Adsorption			Rinse		PEQ1 ↓	PEQ2 ↓	Blowdn	Purge
5	Blowdn	Purge			PEQ2 ↑	PEQ1 ↑	Rep	Adsorption				Rinse		PEQ1 ↓	PEQ2 ↓
6	PEQ1 ↓	PEQ2 ↓	Blowdn	Purge			PEQ2 ↑	PEQ1 ↑	Rep	Adsorption				Rinse	
7	Rinse		PEQ1 ↓	PEQ2 ↓	Blowdn	Purge			PEQ2 ↑	PEQ1 ↑	Rep	Adsorption			
8	Adsorption		Rinse		PEQ1 ↓	PEQ2 ↓	Blowdn	Purge			PEQ2 ↑	PEQ1 ↑	Rep	Adsorption	

Fig. 8. SEWGS cycle for coal syngas with 2 pressure equalisations, using 8 columns (PEQ: pressure equalisation between two columns, Blowdn: blowdown/depressurisation to atmospheric pressure; Rep: repressurisation with hydrogen product).

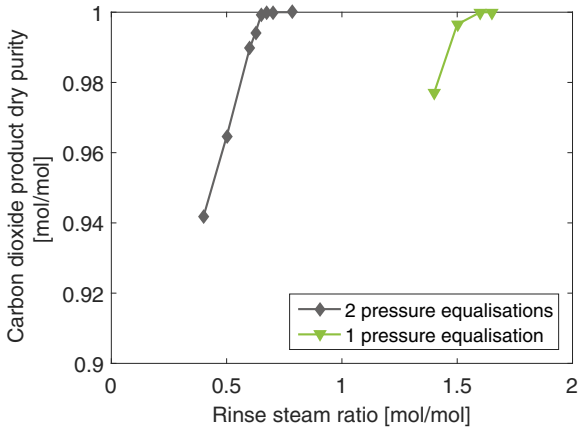

Fig. 9. SEWGS performance, carbon dioxide product dry purity versus rinse steam consumption for natural gas syngas after pre-shift (Walspurger et al., 2015).

S/C_{purge} = 0.4, but only 6 columns are required. Note that this is not only a significant decrease in steam consumption but also in the number of columns required compared to previous cases (cf. the study by Gazzani et al. (2013b) using a 9 columns SEWGS train) (Fig. 10).

For the production of hydrogen fuel (case III and IX), additional dilution was required. Note that SEWGS captures hydrogen sulphide together with carbon dioxide and the concentration of hydrogen sulphide in the carbon dioxide product reaches 3600 ppmv (case III and IV), which exceeds the specification of 200 ppmv (Franco et al., 2009). The sulphur could be recovered as elemental sulphur through the Claus process, but no technology is currently industrially available with sufficient selectivity to produce concentrated hydrogen sulphide from a hydrogen sulphide–carbon dioxide mixture: Selexol or Rectisol are not sufficiently selective to produce concentrated hydrogen sulphide stream required by a Claus process (Kohl and Nielsen, 1997). Gazzani et al. (2013a) have proposed the production of calcium sulphate though stoichiometric combustion of hydrogen sulphide with oxygen. This was predicted to have an energy efficiency penalty of a mere 0.2%-points. Since the current sequestration requirements are subject to ongoing debate, the role of hydrogen sulphide in the carbon dioxide product is not further considered in this work.

3.3. Palladium-based membranes

The membrane modules for hydrogen separation were designed at 70–95% hydrogen recovery. The countercurrent sweep flow rate was adjusted in order to ensure sufficient driving force (cf. Section 2.1.4). The critical point for the driving force turned out to be the sweep inlet of the first membrane module, where the partial pressure of hydrogen in the retentate approached the partial pressure of hydrogen in the sweep (i.e., the hydrogen that permeated in the second and third module). The results of the hydrogen recovery variations are summarised in Table 6. For all of the simulated cases, the optimum efficiency was achieved with a module hydrogen recovery of 80%, which was subsequently used in the further evaluation of the technology. The corresponding overall HRF was in the range of 96.8–99.8% (e.g., ignoring the additional production of hydrogen through interstage WGS, three membrane modules with a hydrogen recovery of 80% each achieve an overall HRF of $1-(1-0.8)^3 = 0.992$).

Table 6
Hydrogen recovery variations for the membrane modules in cases V, VI, XI, and XII.

Case	Module hydrogen recovery [%]	HRF overall [%]	η_0 [%]	η_2 [%]
V	0.95	99.43	88.5	59.8
	0.90	99.18	88.0	69.3
	0.80	98.52	86.3	72.8
	0.70	97.68	83.4	71.9
VI	0.95	99.25	88.5	68.4
	0.90	98.68	88.0	74.1
	0.80	96.78	86.3	76.3
	0.70	93.59	83.4	76.0
XI	0.95	99.98	98.2	88.2
	0.90	99.95	98.2	88.2
	0.80	99.82	98.1	88.2
	0.70	99.59	98.0	88.1
XII	0.95	99.95	81.8	87.4
	0.90	99.80	81.7	88.2
	0.80	98.90	80.9	88.3
	0.70	96.74	79.2	87.6

The amount of sweep gas required was such, that the hydrogen concentration in the product amounted to 38–39 mol% and therefore no additional dilution of the hydrogen fuel product was required in cases V and XI. For the pure hydrogen product in case VI and XII, the hydrogen purity is lower than in the cases based on PSA, but this is only due to the presence of water because of the water dew point (currently assumed 25 °C).

3.4. System efficiencies and work of separation

The results that were summarised in Table 5 are detailed in terms of the relative contributions to the efficiency penalty in Figs. 11–14. The lower heating value (net heating value) multiplied by the feed mass flow rate is scaled to 100, all other contributions are scaled on the same basis. The resulting values of η_0, η_1, and η_2 are also scaled to 100 and plotted in between.

The carbon capture ratio, which is the translation of the rationale behind all these process schemes, is the single most important parameter not yet accounted for in the efficiency comparison in Figs. 11–14. As summarised in Table 5, the carbon capture ratios for the natural gas cases are similar. For the coal syngas cases, the carbon capture ratio for SEWGS (case III and IV) is significantly higher than for the other cases. The achieved carbon capture ratio is plotted in Fig. 15 versus the work of separation, as measured by the loss in theoretical net efficiency.

4. Discussion

The results for the separation of carbon dioxide from hydrogen in the cases defined compare best in several subsets, for coal syngas

Column	1/6		1/6		1/12	1/12	1/12	1/6		1/12	1/12	1/12
1	Adsorption		Rinse		PEQ1 ↓	PEQ2 ↓	Blowdn	Purge		PEQ2 ↑	PEQ1 ↑	Rep
2	PEQ1 ↑	Rep	Adsorption		Rinse		PEQ1 ↓	PEQ2 ↓	Blowdn	Purge		PEQ2 ↑
3	Purge	PEQ2 ↑	PEQ1 ↑	Rep	Adsorption		Rinse		PEQ1 ↓	PEQ2 ↓	Blowdn	Purge
4	Blowdn	Purge		PEQ2 ↑	PEQ1 ↑	Rep	Adsorption		Rinse		PEQ1 ↓	PEQ2 ↓
5	PEQ1 ↓	PEQ2 ↓	Blowdn	Purge		PEQ2 ↑	PEQ1 ↑	Rep	Adsorption		Rinse	

Fig. 10. SEWGS cycle for natural gas reformate with 2 pressure equalisations, using 6 columns (PEQ: pressure equalisation between two columns, Blowdn: blowdown/depressurisation to atmospheric pressure; Rep: repressurisation with hydrogen product).

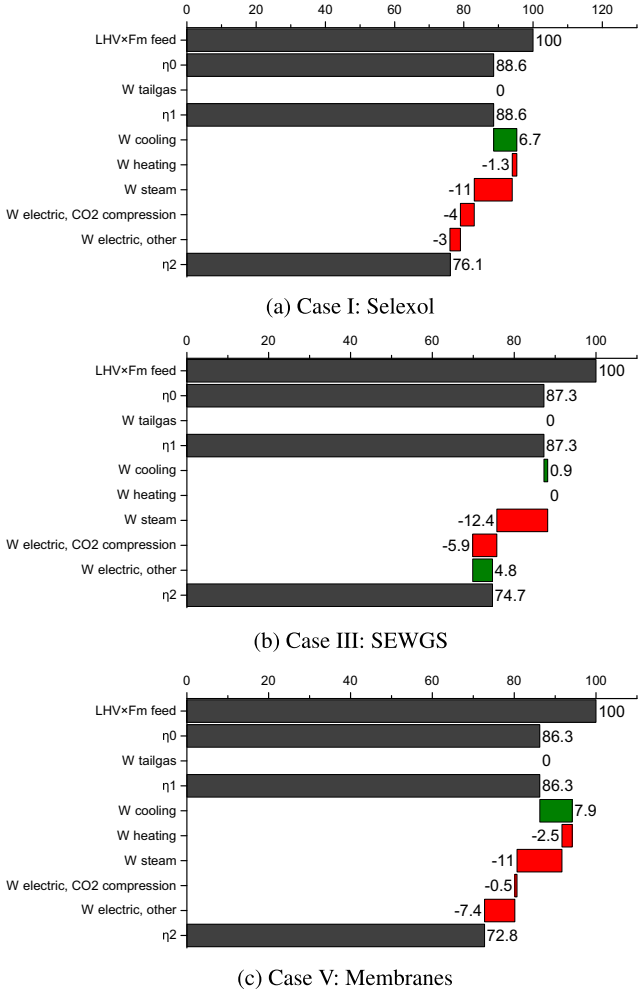

Fig. 11. Efficiency of carbon dioxide capture for coal syngas to decarbonised fuel.

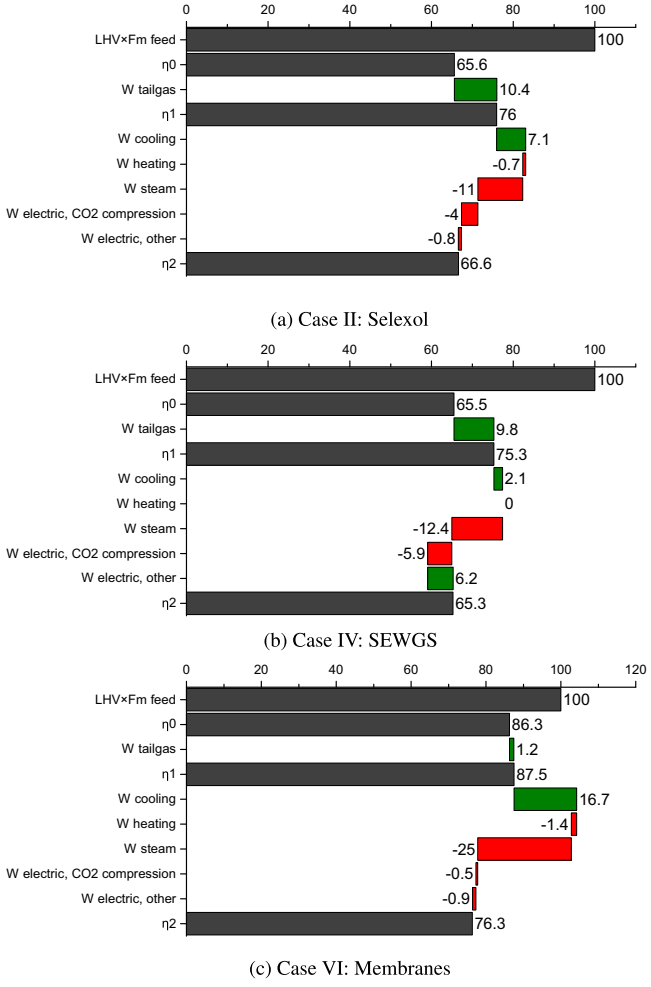

Fig. 12. Efficiency of carbon dioxide capture for coal syngas to hydrogen.

and for natural gas reformate, for decarbonised fuel and for pure hydrogen product.

The current study focuses on the work for carbon dioxide separation, producing hydrogen-rich products from syngas. Therefore, no assessment is made of the efficiency of producing syngas, or of the efficiency with which power can be produced. Regarding the last aspect, it should be noted that the decarbonised fuel product is defined to be used in combined cycle power plants. Alternatively, concentrated hydrogen product streams can be used in fuel cells for power generation (Song, 2002), creating an alternative route for syngas to power with a potentially high efficiency.

4.1. Coal syngas to decarbonised fuel (I, III, V)

For the conversion of coal-derived syngas to hydrogen fuel, conventional Selexol and SEWGS end up with similar net efficiencies η_2, 76% and 75%, respectively (Fig. 11a and b). The reduced cooling and reheating duties that result from the high-temperature operation of SEWGS are clear from the corresponding heating and cooling duties, but this aspect is actually favourable for Selexol (more heat is recovered during cooling than required for reheating). Compared to Selexol, SEWGS requires only 1.4%-points of additional efficiency loss for the addition of steam. Note that the steam requirement of the SEWGS process is calculated using improved understanding of the interaction of carbon dioxide and steam with the sorbent, as discussed by Boon et al. (2015a). The steam consumption has been decreased significantly compared to previous assessments (Gazzani et al., 2013a,b). In addition, a remarkable reduction in capital expenditure has been made with the reduction from 9 to 6 columns, which leads to a decrease in capital expenditure and will further improve the already interesting economic prospects for SEWGS, see e.g. Manzolini et al. (2013). Consequently, further reduction of the SEWGS steam demand (e.g. by increasing the number of pressure equalisations as discussed in Section 2.1.3) is expected to be of little consequence in terms of the overall efficiency penalty. The main advantage of SEWGS, other than the higher carbon capture ratio, appears in the reduced electric work, resulting from the produced work by the two expanders and from avoiding electricity consumption for carbon dioxide capture (in contrast to Selexol).

The membrane route (Fig. 11c) fundamentally differs from the other routes, because hydrogen and not carbon dioxide is captured. Because the carbon dioxide is obtained at high pressure, much less electricity is required for compression of the carbon dioxide product. For case V, as with all membrane cases, the sweep gas use dominates the required work for the separation process (but is necessary for achieving high transmembrane mass flux). It is mainly the compression of nitrogen sweep gas which leads to an electric work input as high as 8%-points in this case, which reduces the theoretical net efficiency to 73%. Optionally, the last membrane stage could be operated at lower pressure to produce low-pressure hydrogen for steam generation, reducing the required membrane surface area and sweep gas compression duty whilst maintaining efficiency (Gazzani et al., 2014b). The use of palladium-alloy instead of pure palladium membranes and the ensuing adoption

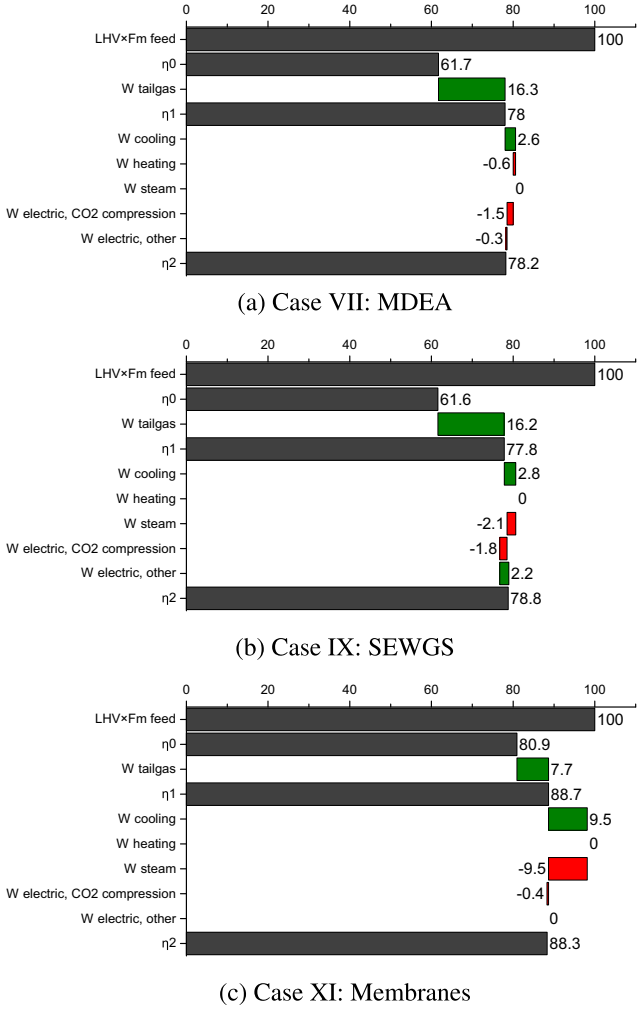

Fig. 13. Efficiency of carbon dioxide capture for natural gas reformate to decarbonised fuel.

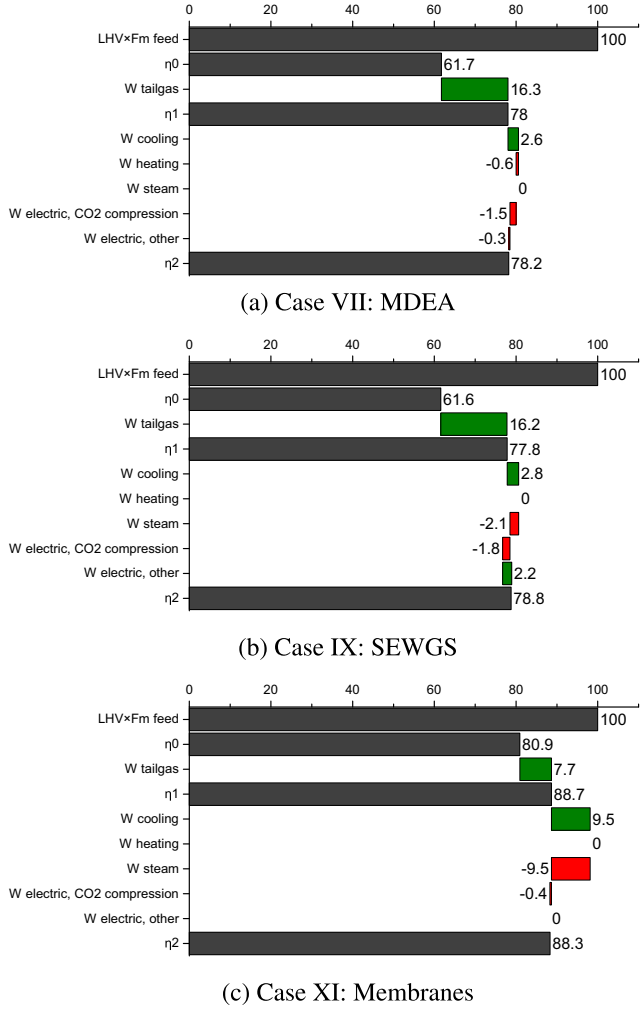

Fig. 14. Efficiency of carbon dioxide capture for natural gas reformate to hydrogen.

of Selexol desulphurisation instead of Rectisol would improve the efficiency (Gazzani and Manzolini, 2015), but only slightly. Of the −8% efficiency penalty for electricity (Fig. 11c), only −0.8%-points are related to the Rectisol process while −6.5%-points are due to nitrogen sweep gas compression. Depending on the plant layout and conditions, operating without sweep and recompression of the hydrogen could present an economically interesting alternative (Koc et al., 2014).

While Selexol has a slightly higher net efficiency ($\eta_2 = 0.76$) than SEWGS ($\eta_2 = 0.75$) and membranes ($\eta_2 = 0.73$), accounting for the strongly enhanced carbon capture rate yields SEWGS as the technology with the lowest efficiency penalty per unit carbon dioxide captured to produce decarbonised fuel from coal syngas. Cormos (2012) predicted a lower efficiency penalty for Selexol, but with a lower carbon capture ratio and a significantly higher efficiency assumption for compression of the carbon dioxide product. The efficiency of Selexol in this work is identical to the efficiency of the Selexol case while for SEWGS the efficiency is slightly lower than the values reported by (Gazzani et al., 2013a) ($\eta_2 = 0.803$), which is related to the SEWGS cycle design. The current cycle design, based on an improved understanding of the interaction of carbon dioxide and steam with the sorbent as discussed in Section 2.1.3, achieves a carbon capture ratio of 98% with $S/C_{rinse} = S/C_{purge} = 0.1$ whereas the cycle used by Gazzani et al. achieves the same capture ratio using $S/C_{rinse} = 0.34$ and $S/C_{purge} = 1.4$. Note that the sorbent in this work is still the alpha-type sorbent and the potential further improvement by using the higher-capacity sorbent beta (Gazzani et al., 2013a) is not yet accounted for.

The pre-combustion capture schemes for IGCC presented here outperform post-combustion capture by absorption from pulverised coal power plants, reaching an efficiency of $\eta_2 = 0.6$ and a target value of $\eta_2 = 0.71$ (House et al., 2009). A recently presented

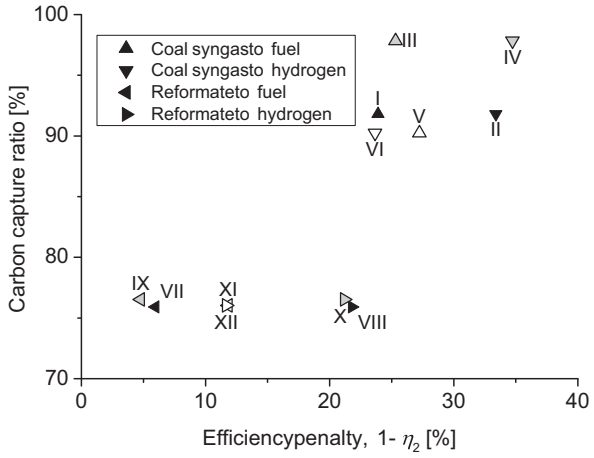

Fig. 15. Comparison of the twelve cases in terms of carbon capture ratio (CCR) versus required efficiency penalty ($1-\eta_2$).

design study reports higher efficiencies, approaching the efficiencies in this work for Selexol and SEWGS with a newly developed solvent, albeit at a lower carbon dioxide capture ratio (Sanchez Fernandez et al., 2014; Manzolini et al., 2015).

4.2. Coal syngas to pure hydrogen (II, IV, VI)

For the conversion of coal-derived syngas to pure hydrogen, conventional Selexol and SEWGS (Fig. 12a and b, respectively) again perform similar in terms of the net efficiency η_2. Their performance suffers equally from the relatively low product recovery in the hydrogen PSA unit, from which the tail gas is used but at an LHV efficiency of 45%. Again SEWGS outperforms Selexol in terms of the efficiency penalty per unit of carbon dioxide captured.

The membrane system (Fig. 12c) performs significantly more efficient than its counterparts, because pure hydrogen can be produced directly (requiring only condensation for water removal). The high work required for generating sweep steam is largely recovered when cooling down the hydrogen-steam mixture from the membrane permeate product. Depending on the plant layout and conditions, operating without sweep and recompression of the hydrogen could present an economically interesting alternative (Ma et al., 2015). Although the remaining net work for producing the sweep stream is still the largest contribution to the efficiency penalty, membranes represent the most efficient technology for the production of pure hydrogen from coal syngas.

4.3. Natural gas reformate to decarbonised fuel (VII, IX, XI)

For the conversion of natural gas reformate to hydrogen fuel, SEWGS (Fig. 13b) has a higher net efficiency η_2 than MDEA (Fig. 13a). The theoretical net efficiency penalty for MDEA is 6%, while the overall system efficiency penalty of carbon dioxide capture by MDEA in NGCC typically reaches 16% (8%-points) (Jansen et al., 2015). As for the coal cases, the net effect of cooling down and reheating of the process gas is slightly favourable for MDEA, because more heat is recovered in the cooling than is required for reheating. Conversely, the SEWGS-based process requires 2.7%-points less electricity; in the SEWGS flowsheet, the expanders result in a net electricity production. Compared to the prediction by Cobden et al. (2007), the steam consumption has been reduced and the efficiency penalty $(1-\eta_2)$ for SEWGS has been reduced from up to 12% to 5% which is much closer to the minimum value of 2.7%. Gazzani et al. (2013b) also reported a slightly higher efficiency for SEWGS compared to MDEA. As for the cases above, the membrane case (Fig. 13c) has the lowest theoretical net efficiency which is a result of the work required for raising sweep steam. Note that the low capture ratio is not due to the employed separation processes but instead due to the methane conversion assumed, as witnessed from the carbon oxides capture ratio in Table 5. Post-combustion capture would in principle allow for higher carbon capture ratios because it allows to also capture part of the carbon dioxide that is produced by the combustion of PSA offgas, but Iyer et al. (2015a) found 66.5% CCR because carbon dioxide was not captured from the capture unit boiler. Of the carbon (carbon monoxide, carbon dioxide, and methane) in the reformate, 19 mol% is methane which can be used to underfire the reformer (Rostrup-Nielsen, 1993; Molburg and Doctor, 2003; Rath, 2010) and is thus not captured. In the MDEA and SEWGS cases for fuel, the methane ends up in the hydrogen fuel to be combusted. In the membranes case (XI) to fuel, the cryogenic process for carbon dioxide purification recovers the methane which is mixed with the hydrogen fuel. Based on carbon oxides only, MDEA and palladium-based membrane achieve a CO_xCR of 94% while SEWGS would achieve 95%.

Outside the scope of the current study, in the case of natural gas reformate to power, post-combustion carbon dioxide capture could be preferred from a thermodynamic efficiency point of view (Gazzani et al., 2013b), although a recent study found an efficiency penalty of 12% for carbon dioxide capture in NGCC (Iyer et al., 2015b), which is higher than the currently predicted efficiency penalties for MDEA (case VII) and SEWGS (case IX). Still, newly developed amine solvents could reduce the efficiency penalty for post-combustion carbon dioxide capture (Manzolini et al., 2015).

Because it yields the highest efficiency as well as the highest carbon capture ratio, SEWGS is the most efficient process to produce decarbonised fuel from natural gas reformate.

4.4. Natural gas reformate to pure hydrogen (VIII, X, XII)

For the conversion of natural gas reformate to pure hydrogen, conventional MDEA and SEWGS (Fig. 14a and b, respectively) have a similar net efficiency with an advantage for SEWGS. The efficiencies are largely determined by the performance of the PSA system for the production of pure hydrogen, as in the corresponding coal syngas cases. In the MDEA and SEWGS cases for hydrogen, the methane is recovered in the PSA tail gas as accounted for in the models. In the membranes case (XII) the methane is recovered in the cryogenic carbon dioxide purification and accounted for as fuel. Again, the inherent advantage of palladium membranes producing pure hydrogen is reflected in the much higher net efficiencies (Fig. 14c), more than compensating for the work required for raising sweep steam.

The introduction of membrane water–gas shift reactor technology, instead of staged water–gas shift and membrane modules, could further improve the efficiency of the system (Gallucci et al., 2013; van Berkel et al., 2013; Fernandez et al., 2015), although it should be noted that the carbon monoxide conversion after three stages with 95% hydrogen recovery factor is already 99.9 mol% and the amount of sweep gas is probably not significantly reduced by the adoption of integrated membrane reactor technology. Outside the scope of the current work, the integrated membrane reactor technology might benefit from a lower capital expenditure.

With the highest theoretical net efficiency, membranes are the most efficient technology for the production of pure hydrogen from natural gas reformate.

5. Conclusions

Sorption-enhanced water–gas shift (SEWGS) and palladium-based membranes have been compared to conventional technologies for hydrogen-carbon dioxide separation based on the carbon capture ratio and energy efficiency penalty. Four major process routes were assessed, each leading to different conclusions.

- For the production of decarbonised fuel from coal syngas, SEWGS yields the lowest efficiency penalty per unit of carbon dioxide captured.
- For the production of pure hydrogen from coal syngas, SEWGS has a significantly higher carbon capture ratio than the alternatives while palladium membranes yield the lowest efficiency penalty per unit of carbon dioxide captured.
- For the production of decarbonised fuel from natural gas reformate, SEWGS is the most efficient technology in terms of efficiency penalty.
- For the production of pure hydrogen from natural gas syngas, palladium membranes yield the lowest efficiency penalty.

Acknowledgements

The authors gratefully acknowledge fruitful discussions with Wim Haije (TUDelft) and Jaap Vente (ECN). Stephen Peper

performed the SEWGS simulations at ECN in cooperation with Paul Cobden (ECN) and Eric van Dijk (ECN), who are kindly acknowledged for their contributions. Part of this research has been carried out in the context of the CATO-2 programme. CATO-2 is the Dutch national research programme on CO_2 Capture and Storage technology (CCS). The programme is financially supported by the Dutch Government (Ministry of Economic Affairs) and the Industrial CATO-2 Consortium Parties.

References

Atsonios, K., Koumanakos, A.K., Panopoulos, K.D., Doukelis, A., Kakaras, E., 2015. 12 – using palladium membranes for carbon capture in natural gas combined cycle (NGCC) power plants: process integration and techno-economics. In: Doukelis, A., Panopoulos, K., Koumanakos, A., Kakaras, E. (Eds.), Palladium Membrane Technology for Hydrogen Production, Carbon Capture and Other Applications (Woodhead Publishing Series in Energy). Woodhead Publishing, Cambridge, UK, pp. 247–285, http://dx.doi.org/10.1533/9781782422419.2.247.

Atsonios, K., Panopoulos, K.D., Doukelis, A., Koumanakos, A., Kakaras, E., 2013. Cryogenic method for H_2 and CH_4 recovery from a rich CO_2 stream in pre-combustion carbon capture and storage schemes. Energy 53, 106–113, http://dx.doi.org/10.1016/j.energy.2013.02.026.

Basile, A., Gallucci, F., Tosti, S., 2008. Synthesis, characterization and applications of palladium membranes. Membr. Sci. Technol. 13, 255–323, 10.1016/S0927-5193(07)13008-4.

Beavis, R., 2011. The EU FP6 CACHET project – final results. Energy Proc. 4, 1074–1081, http://dx.doi.org/10.1016/j.egypro.2011.01.157.

van Berkel, F., Hao, C., Bao, C., Jiang, C., Xu, H., Morud, J., Peters, T., Soutif, E., Dijkstra, J.W., Jansen, D., Song, B., 2013. Pd-membranes on their way towards application for CO_2-capture. Energy Proc. 37, 1076–1084, http://dx.doi.org/10.1016/j.egypro.2013.05.204.

Boll, W., Hochgesand, G., Higman, C., Supp, E., Kalteier, P., Müller, W.D., Kriebel, M., Schlichting, H., Tanz, H., 2000. Gas production 3. Gas treating. In: Ullmann's Encyclopedia of Industrial Chemistry. Wiley-VCH, Weinheim, Germany, pp. 483–539, http://dx.doi.org/10.1002/14356007.o12_o02.

Boon, J., Cobden, P.D., van Dijk, H.A.J., Hoogland, C., van Selow, E.R., van Sint Annaland, M., 2014. Isotherm model for high-temperature, high-pressure adsorption of CO_2 and H_2O on K-promoted hydrotalcite. Chem. Eng. J. 248, 406–414, http://dx.doi.org/10.1016/j.cej.2014.03.056.

Boon, J., Cobden, P.D., van Dijk, H.A.J., van Sint Annaland, M., 2015a. High-temperature pressure swing adsorption cycle design for sorption-enhanced water–gas shift. Chem. Eng. Sci. 122, 219–231, http://dx.doi.org/10.1016/j.ces.2014.09.034.

Boon, J., van Dijk, E., Pirgon-Galin, O., Haije, W., van den Brink, R., 2009. Water–gas shift kinetics over FeCr-based catalyst: effect of hydrogen sulphide. Catal. Lett. 131, 406–412, http://dx.doi.org/10.1007/s10562-009-0090-0.

Boon, J., Pieterse, J.A.Z., van Berkel, F.P.F., van Delft, Y.C., van Sint Annaland, M., 2015b. Hydrogen permeation through palladium membranes and inhibition by carbon monoxide, carbon dioxide, and steam. J. Membr. Sci. 496, 344–358, http://dx.doi.org/10.1016/j.memsci.2015.08.061.

Boon, J., Pieterse, J.A.Z., Dijkstra, J.W., van Delft, Y.C., Veenstra, P., Nijmeijer, A., Jansen, D., 2013. Benchmarking of hydrogen selective membranes: experimental and modelling approach to compare membrane performance. Energy Proc. 37, 1020–1029, http://dx.doi.org/10.1016/j.egypro.2013.05.198.

Boon, J., Pieterse, J.A.Z., Dijkstra, J.W., van Sint Annaland, M., 2012. Modelling and systematic experimental investigation of mass transfer in supported palladium-based membrane separators. Int. J. Greenh. Gas Control 11, 122–129, http://dx.doi.org/10.1016/j.ijggc.2012.09.014.

Bracht, M., Alderliesten, P.T., Kloster, R., Pruschek, R., Haupt, G., Xue, E., Ross, J.R.H., Koukou, M.K., Papayannakos, N., 1997. Water gas shift membrane reactor for CO_2 control in IGCC systems: techno-economic feasibility study. Energy convers. Manage. 38, S159–S164, http://dx.doi.org/10.1016/S0196-8904(96)00263-4.

Carbo, M.C., Boon, J., Jansen, D., van Dijk, H.A.J., Dijkstra, J.W., van den Brink, R.W., Verkooijen, A.H.M., 2009. Steam demand reduction of water–gas shift reaction in IGCC power plants with pre-combustion CO_2 capture. Int. J. Greenh. Gas Control 3, 712–719, http://dx.doi.org/10.1016/j.ijggc.2009.08.003.

Carbo, M.C., Smit, R., van der Drift, B., Jansen, D., 2011. Bio energy with CCS (BECCS): large potential for BioSNG at low CO_2 avoidance cost. Energy Proc. 4, 2950–2954, http://dx.doi.org/10.1016/j.egypro.2011.02.203.

Cau, G., Tola, V., Deiana, P., 2014. Comparative performance assessment of USC and IGCC power plants integrated with CO_2 capture systems. Fuel 116, 820–833, http://dx.doi.org/10.1016/j.fuel.2013.06.005.

Chiesa, P., Campanari, S., Manzolini, G., 2011. CO_2 cryogenic separation from combined cycles integrated with molten carbonate fuel cells. Int. J. Hydrogen Energy 36, 10355–10365, http://dx.doi.org/10.1016/j.ijhydene.2010.09.068.

Chiesa, P., Macchi, E., 2004. A thermodynamic analysis of different options to break 60% electric efficiency in combined cycle power plants. J. Eng. Gas Turbines Power 126, 770–785, http://dx.doi.org/10.1115/1.1771684.

Chiesa, P., Romano, M.C., Spallina, V., Turi, D.M., Mancuso, L., 2013. Efficient low CO_2 emissions power generation by mixed conducting membranes. Energy Proc. 37, 905–913, http://dx.doi.org/10.1016/j.egypro.2013.05.185.

Cobden, P.D., van Beurden, P., Reijers, H.T.J., Elzinga, G.D., Kluiters, S.C.A., Dijkstra, J.W., Jansen, D., van den Brink, R.W., 2007. Sorption-enhanced hydrogen production for pre-combustion CO_2 capture: thermodynamic analysis and experimental results. Int. J. Greenh. Gas Control 1, 170–179, http://dx.doi.org/10.1016/S1750-5836(07)00021-7.

Cormos, C.C., 2012. Integrated assessment of IGCC power generation technology with carbon capture and storage (CCS). Energy 42, 434–445, http://dx.doi.org/10.1016/j.energy.2012.03.025.

van Dijk, H.A.J., Cohen, D., Hakeem, A.A., Makkee, M., Damen, K., 2014. Validation of a water–gas shift reactor model based on a commercial FeCr catalyst for pre-combustion CO_2 capture in an IGCC power plant. Int. J. Greenh. Gas Control 29, 82–91, http://dx.doi.org/10.1016/j.ijggc.2014.07.005.

van Dijk, H.A.J., Walspurger, S., Cobden, P.D., van den Brink, R.W., de Vos, F.G., 2011. Testing of hydrotalcite-based sorbents for CO_2 and H_2S capture for use in sorption enhanced water gas shift. Int. J. Greenh. Gas Control 5, 505–511, http://dx.doi.org/10.1016/j.ijggc.2010.04.011.

Dijkstra, J.W., Pieterse, J.A.Z., Li, H., Boon, J., van Delft, Y.C., Raju, G., Peppink, G., van den Brink, R.W., Jansen, D., 2011. Development of membrane reactor technology for power production with pre-combustion CO_2 capture. Energy Proc. 4, 715–722, http://dx.doi.org/10.1016/j.egypro.2011.01.110.

Fernandez, E., Helmi, A., Coenen, K., Melendez, J., Viviente, J.L., Tanaka, D.A.P., van Sint Annaland, M., Gallucci, F., 2015. Development of thin Pd-Ag supported membranes for fluidized bed membrane reactors including WGS related gases. Int. J. Hydrogen Energy 40, 3506–3519, http://dx.doi.org/10.1016/j.ijhydene.2014.08.074.

Franco, A., Russo, A., 2002. Combined cycle plant efficiency increase based on the optimization of the heat recovery steam generator operating parameters. Int. J. Thermal Sci. 41, 843–859, http://dx.doi.org/10.1016/S1290-0729(02)01378-9.

Franco, F., Bolland, O., Booth, N., Macchi, E., Manzolini, G., Naqvi, R., Pfeffer, A., Rezvani, S., Abu Zara, M., 2009. Common Framework Definition Document. Technical Report D4.6. European Benchmarking Task Force. http://caesar.ecn.nl/fileadmin/caesar/user/documents/D4. 6-Common_Framework-final.pdf.

Gallucci, F., Fernandez, E., Corengia, P., van Sint Annaland, M., 2013. Recent advances on membranes and membrane reactors for hydrogen production. Chem. Eng. Sci. 92, 40–66, http://dx.doi.org/10.1016/j.ces.2013.01.008.

Gazzani, M., Chiesa, P., Martelli, E., Sigali, S., Brunetti, I., 2014a. Using hydrogen as gas turbine fuel: premixed versus diffusive flame combustors. J. Eng. Gas Turbines Power 136, 051504, http://dx.doi.org/10.1115/1.4026085.

Gazzani, M., Macchi, E., Manzolini, G., 2013a. CO_2 capture in integrated gasification combined cycle with SEWGS – Part A: Thermodynamic performances. Fuel 105, 206–219, http://dx.doi.org/10.1016/j.fuel.2012.07.048.

Gazzani, M., Macchi, E., Manzolini, G., 2013b. CO_2 capture in natural gas combined cycle with SEWGS. Part A: Thermodynamic performances. Int. J. Greenh. Gas Control 12, 493–501, http://dx.doi.org/10.1016/j.ijggc.2012.06.010.

Gazzani, M., Manzolini, G., 2015. 11 – using palladium membranes for carbon capture in integrated gasification combined cycle (IGCC) power plants. In: Doukelis, A., Panopoulos, K., Koumanakos, A., Kakaras, E. (Eds.), Palladium Membrane Technology for Hydrogen Production, Carbon Capture and Other Applications (Woodhead Publishing Series in Energy). Woodhead Publishing, Cambridge, UK, pp. 221–246, http://dx.doi.org/10.1533/9781782422419.2.221.

Gazzani, M., Romano, M.C., Manzolini, G., 2015. CO_2 capture in integrated steelworks by commercial-ready technologies and SEWGS process. Int. J. Greenh. Gas Control 41, 249–267, http://dx.doi.org/10.1016/j.ijggc.2015.07.012.

Gazzani, M., Turi, D.M., Manzolini, G., 2014b. Techno-economic assessment of hydrogen selective membranes for CO_2 capture in integrated gasification combined cycle. Int. J. Greenh. Gas Control 20, 293–309, http://dx.doi.org/10.1016/j.ijggc.2013.11.006.

Gielen, D., 2003. CO_2 removal in the iron and steel industry. Energy Convers. Manage. 44, 1027–1037, http://dx.doi.org/10.1016/S0196-8904(02)00111-5.

Häussinger, P., Lohmüller, R., Watson, A.M., 2012. Hydrogen, 2. Production. In: Ullmann's Encyclopedia of Industrial Chemistry. Wiley-VCH, Weinheim, Germany, pp. 249–307, http://dx.doi.org/10.1002/14356007.o13_o03.

Häussinger, P., Lohmüller, R., Watson, A.M., 2012. Hydrogen, 6. Uses. In: Ullmann's Encyclopedia of Industrial Chemistry. Wiley-VCH, Weinheim, Germany, pp. 353–392, http://dx.doi.org/10.1002/14356007.o13_o07.

Holladay, J.D., Hu, J., King, D.L., Wang, Y., 2009. An overview of hydrogen production technologies. Catal. Today 139, 244–260, http://dx.doi.org/10.1016/j.cattod.2008.08.039.

House, K.Z., Harvey, C.F., Aziz, M.J., Schrag, D.P., 2009. The energy penalty of post-combustion CO_2 capture & storage and its implications for retrofitting the US installed base. Energy Environ. Sci. 2, 193–205, http://dx.doi.org/10.1039/B811608C.

Hudiono, Y., Whitlock, M., Jadhav, R., 2015. Development of palladium alloy membrane for H_2 recovery from autothermal reformers. In: Gerdes, K.F. (Ed.), Carbon Dioxide Capture for Storage in Deep Geological Formations, vol. 4. CPL, Thatcham, UK, pp. 111–124 (chapter 10).

Hufton, J.R., Mayorga, S., Sircar, S., 1999. Sorption-enhanced reaction process for hydrogen production. AIChE J. 45, 248–256.

Iyer, M., Beavis, R., Tarrant, T., Bullen, T., Butler, D., 2015a. Techno-economic assessment of deep CO_2 capture from hydrogen plants. In: Gerdes, K.F. (Ed.), Carbon Dioxide Capture for Storage in Deep Geological Formations, vol. 4. CPL, Thatcham, UK, pp. 153–164 (chapter 12).

Iyer, M., Beavis, R., Tarrant, T., Bullen, T., Butler, D., 2015b. Techno-economic assessment of power generation from natural gas in combined cycle (NGCC) systems with integrated capture. In: Gerdes, K.F. (Ed.), Carbon Dioxide Capture

for Storage in Deep Geological Formations, vol. 4. CPL, Thatcham, UK, pp. 317–328 (chapter 22).
Jansen, D., Gazzani, M., Manzolini, G., van Dijk, E., Carbo, M., 2015. Pre-combustion CO_2 capture. Int. J. Greenh. Gas Control 40, 167–187, http://dx.doi.org/10.1016/j.ijggc.2015.05.028, Special Issue commemorating the 10th year anniversary of the publication of the Intergovernmental Panel on Climate Change Special Report on CO_2 Capture and Storage.
Jansen, D., van Selow, E., Cobden, P., Manzolini, G., Macchi, E., Gazzani, M., Blom, R., Henriksen, P.P., Beavis, R., Wright, A., 2013. SEWGS technology is now ready for scale-up! Energy Proc. 37, 2265–2273, http://dx.doi.org/10.1016/j.egypro.2013.06.107.
Koc, R., Kazantzis, N.K., Ma, Y.H., 2014. Membrane technology embedded into IGCC plants with CO_2 capture: an economic performance evaluation under uncertainty. Int. J. Greenh. Gas Control 26, 22–38, http://dx.doi.org/10.1016/j.ijggc.2014.04.004.
Kohl, A.L., Nielsen, R., 1997. Gas Purification. Gulf, Houston TX, USA.
Lee, W.Y., Kim, S.S., 1992. The maximum power from a finite reservoir for a Lorentz cycle. Energy 17, 275–281, http://dx.doi.org/10.1016/0360-5442(92)90055-5.
Li, H., Dijkstra, J.W., Pieterse, J.A.Z., Boon, J., van den Brink, R.W., Jansen, D., 2010. Towards full-scale demonstration of hydrogen-selective membranes for CO_2 capture: inhibition effect of WGS-components on the H_2 permeation through three Pd membranes of 44 cm long. J. Membr. Sci. 363, 204–211, http://dx.doi.org/10.1016/j.memsci.2010.07.029.
Li, H., Dijkstra, J.W., Pieterse, J.A.Z., Boon, J., van den Brink, R.W., Jansen, D., 2011. WGS-mixture separation and WGS reaction test in a bench-scale multi-tubular membrane reactor. Energy Proc. 4, 666–673, http://dx.doi.org/10.1016/j.egypro.2011.01.103.
Li, H., Pieterse, J.A.Z., Dijkstra, J.W., Boon, J., van den Brink, R.W., Jansen, D., 2012. Bench-scale WGS membrane reactor for CO_2 capture with co-production of H_2. Int. J. Hydrogen Energy 37, 4139–4143, http://dx.doi.org/10.1016/j.ijhydene.2011.11.135.
Ma, L.C., Castro-Dominguez, B., Kazantzis, N.K., Ma, Y.H., 2015. Integration of membrane technology into hydrogen production plants with CO_2 capture: an economic performance assessment study. Int. J. Greenh. Gas Control 42, 424–438, http://dx.doi.org/10.1016/j.ijggc.2015.08.019.
Manzolini, G., Macchi, E., Gazzani, M., 2013. CO_2 capture in integrated gasification combined cycle with SEWGS – Part B: Economic assessment. Fuel 105, 220–227, http://dx.doi.org/10.1016/j.fuel.2012.07.043.
Manzolini, G., Sanchez Fernandez, E., Rezvani, S., Macchi, E., Goetheer, E.L.V., Vlugt, T.J.H., 2015. Economic assessment of novel amine based CO_2 capture technologies integrated in power plants based on European Benchmarking Task Force methodology. Appl. Energy 138, 546–558, http://dx.doi.org/10.1016/j.apenergy.2014.04.066.
Molburg, J.C., Doctor, R.D., 2003. Hydrogen from steam-methane reforming with CO_2 capture. In: 20th Annual International Pittsburgh Coal Conference.
Newsome, D.S., 1980. The water–gas shift reaction. Catal. Rev. Sci. Eng. 21, 275–318, http://dx.doi.org/10.1080/03602458008067535.
Ockwig, N.W., Nenoff, T.M., 2007. Membranes for hydrogen separation. Chem. Rev. 107, 4078–4110, http://dx.doi.org/10.1021/cr0501792.
Paglieri, S.N., Way, J.D., 2002. Innovations in palladium membrane research. Sep. Purif. Rev. 31, 1–169, http://dx.doi.org/10.1081/SPM-120006115.
Patil, C.S., van Sint Annaland, M., Kuipers, J.A.M., 2007. Fluidised bed membrane reactor for ultrapure hydrogen production via methane steam reforming: experimental demonstration and model validation. Chem. Eng. Sci. 62, 2989–3007, http://dx.doi.org/10.1016/j.ces.2007.02.022.
Peng, D.Y., Robinson, D.B., 1976. A new two-constant equation of state. Ind. Eng. Chem. Fundam. 15, 59–64, http://dx.doi.org/10.1021/i160057a011.
Rath, L.K., 2010. Assessment of hydrogen production with CO_2 capture. Volume 1: Baseline state-of-the-art plants. DoE/NETL, report.
Reijers, H.T.J., Boon, J., Elzinga, G.D., Cobden, P.D., Haije, W.G., Brink, R.W.v.d., 2009. Modeling study of the sorption-enhanced reaction process for CO_2 capture. II. Application to steam-methane reforming. Ind. Eng. Chem. Res. 48, 6975–6982, http://dx.doi.org/10.1021/ie8013204.
Rostrup-Nielsen, J.R., 1993. Production of synthesis gas. Catal. Today 18, 305–324, http://dx.doi.org/10.1016/0920-5861(93)80059-A.
Sanchez Fernandez, E., Goetheer, E.L.V., Manzolini, G., Macchi, E., Rezvani, S., Vlugt, T.J.H., 2014. Thermodynamic assessment of amine based CO_2 capture technologies in power plants based on European Benchmarking Task Force methodology. Fuel 129, 318–329, http://dx.doi.org/10.1016/j.fuel.2014.03.042.
van Selow, E.R., Cobden, P.D., van Dijk, H.A.J., Walspurger, S., Verbraeken, P.A., Jansen, D., 2013. Qualification of the ALKASORB sorbent for the sorption-enhanced water–gas shift process. Energy Proc. 37, 180–189, http://dx.doi.org/10.1016/j.egypro.2013.05.100.
van Selow, E.R., Cobden, P.D., Verbraeken, P.A., Hufton, J.R., van Den Brink, R.W., 2009. Carbon capture by sorption-enhanced water–gas shift reaction process using hydrotalcite-based material. Ind. Eng. Chem. Res. 48, 4184–4193, http://dx.doi.org/10.1021/ie801713a.
Song, C., 2002. Fuel processing for low-temperature and high-temperature fuel cells: challenges, and opportunities for sustainable development in the 21st century. Catal. Today 77, 17–49, http://dx.doi.org/10.1016/S0920-5861(02)00231-6.
Spallina, V., Romano, M.C., Chiesa, P., Gallucci, F., van Sint Annaland, M., Lozza, G., 2014. Integration of coal gasification and packed bed CLC for high efficiency and near-zero emission power generation. Int. J. Greenh. Gas Control 27, 28–41, http://dx.doi.org/10.1016/j.ijggc.2014.04.029.
Stepwise, 2016. The Stepwise Project. http://www.stepwise.eu/.
Tiemersma, T.P., Patil, C.S., van Sint Annaland, M., Kuipers, J.A.M., 2006. Modelling of packed bed membrane reactors for autothermal production of ultrapure hydrogen. Chem. Eng. Sci. 61, 1602–1616, http://dx.doi.org/10.1016/j.ces.2005.10.004.
Walspurger, S., Boon, J., Peper, S., Cobden, P.D., van Dijk, H.A.J., Overwater, K., 2015. Process intensification is the key to CO_2 emission abatement: options for steam reforming to hydrogen. In: Presented at the 10th European Congress of Chemical Engineering.
Wang, J., Huang, L., Yang, R., Zhang, Z., Wu, J., Gao, Y., Wang, Q., O'Hare, D., Zhong, Z., 2014. Recent advances in solid sorbents for CO_2 capture and new development trends. Energy Environ. Sci. 7, 3478–3518.
Yong, Z., Mata, V., Rodrigues, A.E., 2002. Adsorption of carbon dioxide at high temperature – a review. Sep. Purif. Technol. 26, 195–205, http://dx.doi.org/10.1016/S1383-5866(01)00165-4.
Yun, S., Oyama, S.T., 2011. Correlations in palladium membranes for hydrogen separation: a review. J. Membr. Sci. 375, 28–45, http://dx.doi.org/10.1016/j.memsci.2011.03.057.

ECN
Westerduinweg 3
1755 LE Petten
The Netherlands

P.O. Box 1
1755 LG Petten
The Netherlands

T +31 88 515 4949
F +31 88 515 8338
info@ ecn.nl
www.ecn.nl